SHOCK TUBE OPERATION, FLOW MODELING AND THEORETICAL ANALYSIS

Mantovani, A. F., eitra13@gmail.com
Romanelli Pinto D., davidromanelli@ieav.cta.br
Collaborators at the Instituto de Estudos Avançados, Trevo Coronel Aviador José Alberto Albano do Amarante, nº 1 Putim 12.228-001 São José dos Campos, SP, Brasil
Undergraduate students of the Faculdade de Tecnologia (FATEC) and ETEP Faculdades (Manufacture of Aeronautical Systems and Mechanical Engineering, respectively)

Toro, P. G. P., toro@ieav.cta.br
Minucci, M. A. S., sala@ieav.cta.br
Instituto de Estudos Avançados, Trevo Coronel Aviador José Alberto Albano do Amarante, nº 1 Putim 12.228-001 São José dos Campos, SP, Brasil

Abstract. *Shock tubes have been extensively used to investigate many special problems those arise in various fields such chemistry, physics, fluid dynamics, structures and astrophysics. In particular, they have been widely used for high speed and high temperature research since the early 1950s for studies of aerodynamics. Therefore, they are the most versatile experimental short duration ground test facilities, which provide high enthalpy flows close to those encountered during the reentry of a space vehicle into the earth's atmosphere at hypersonic flight speeds. The simplest shock tubes consist basically of a driver and a driven sections, with constant area, separated by a single thin diaphragm. The diaphragm allows one to maintain different pressure in each tube. When the diaphragm is suddenly ruptured at the select high pressure in the driver section, compression waves are generated which coalesce into a normal shock wave. This shock then propagates into the low-pressure driven section while an expansion or rarefaction wave is propagated into the high-pressure driver section. The shock wave arrives at the end wall of the driven section and it is totally reflected. Different gases at different temperatures can be used in the driver and driven sections. The quasi-steady motion may be studied around the model housed in the test section, which is placed at the end or close to the end of the driven section. The one-dimensional incident shock wave moving into a stationary gas and the reflect shock wave mode may be used to calculate the flow conditions in the shock tube and the flow over the test model. The flow modeling of the properties downstream of the shock wave for the simplest shock tube is being presented considering different gases at same initial ambient temperatures used in the driver and driven sections. Theoretical analysis is presented for calorically perfect gas assumption, which the properties downstream of the shock wave are functions only of the flow Mach number, the gas and the properties upstream of the shock wave. Special measurement techniques to measure pressure and temperature (heat flux) must be developed for the short running time shock tube and examples of the pressure and the temperature (heat flux) calibrations using the IEAv 0.65-mm. diameter low-pressure shock tube are presented.*

Keywords*: shock tube, hypersonic facility, shock tube modeling, shock tube theoretical analysis*

1. INTRODUCTION

Shock tubes and shock tunnels are the most versatile experimental short duration facilities. They have been widely used for high velocity and high temperature research since the early 1950s. Both shock tubes and shock tunnels are ground test facilities which provide high enthalpy flows close to those encountered during the reentry of a space vehicle into the earth's atmosphere at hypersonic flight speeds. These short running time facilities require special measurement techniques to measure pressure and temperature (heat flux) for the models in the test section.

Lukasiewicz (1952), Nagamatsu (1958, 1961) and Glass and Hall (1959) comment the shock tube was first used by Vielle in France in 1899 to investigate the flame propagation problem. Vielle measured shock velocities up to about twice the velocity of sound in the atmospheric air. From that time, shock tubes have been used extensively to investigate many special problems that arise in various fields such chemistry, physics, fluid dynamics, structures and astrophysics. The ability of the shock tube to simulate the high temperature and velocities of the hypersonic flight has led to its widespread use as a primary tool for high-temperature gasdynamic research. The shock tunnel consists of a shock tube with a nozzle attached to the end of the tube to produce higher flow Mach numbers with higher stagnation temperatures in the test section (Nagamatsu, 1958, 1961).

Since the ability to conduct ground tests at high flight Mach numbers and high enthalpies are limited, expensive flight experiments are also used to design the hypersonic vehicles. An increase in the capability of existing ground test facilities is necessary to reduce the number of required flight tests. Also, the fundamental knowledge necessary for complex flow phenomena at hypersonic flows may be analyzed by the Computational Fluid Dynamic (CFD). But a combination of CFD and experimental investigations that simulate the Mach numbers and the enthalpies for the

hypersonic flight conditions is necessary. The experimental data (by ground test facilities and by flight tests) should define the physics of the hypersonic flow phenomena to validate or to modify the available CFD codes.

In this work only the theory of the shock tube is given in some detail in a convenient form to investigate the aerodynamic design of the shock tube and the compressible flow.

2. SHOCK TUBE OPERATION

The simplest of shock tube consists basically of driver and driven sections, with constant area, separated by a single thin diaphragm. The diaphragm allows one to maintain different pressure in each section, Fig. 1.

When the diaphragm is suddenly ruptured at the select high pressure in the driver section, compression waves are generated which coalesce into a normal shock wave. This shock then propagates into the low-pressure driven section, while an expansion or rarefaction wave is propagated into the high-pressure driver section. The shock wave arrives at the end wall of the driven section and it is reflected totally. Different gases at different temperatures may be used in the driver and driven sections. The quasi-steady motion may be studied around the model housed in the test section, which is placed at the end or close to the end of the driven section.

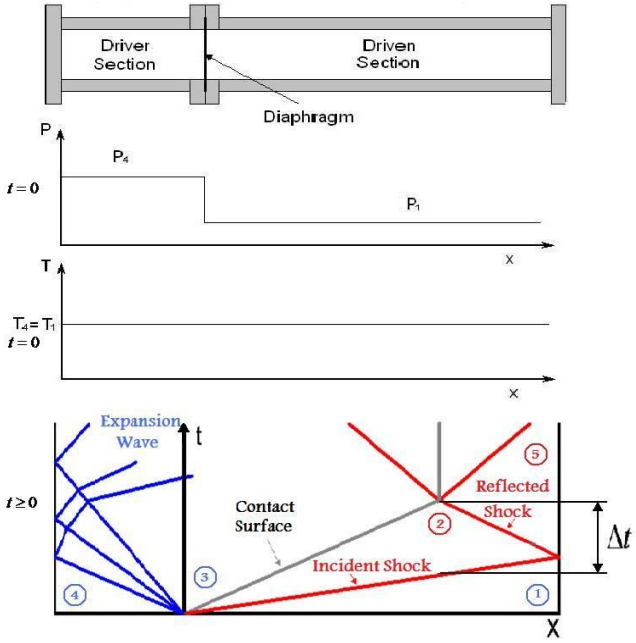

Figure 1. Constant cross section area shock tube, initial conditions and wave diagram for a shock tube.

Thermodynamic properties, in equilibrium, as well as the velocities of the gases, pressurized in the driver and driven sections, at high pressure and low pressure, are identified by the index (4) and (1), respectively.

Initially, Fig. 1, the low-pressure section, known as driven, is pressurized, isentropically at ambient temperature, T_1, with pressure, p_1, while the high pressure section, known as a driver, is pressurized, isentropically at ambient temperature, T_4, with pressure, p_4. Therefore, in $t = 0$ the system is in equilibrium thermodynamic, $T_4 = T_1$.

Ideally, at $t = 0$, Fig. 2, when the diaphragm is broken, the gas in the high pressure section expands toward the low-pressure section, causing the establishment of a normal shock wave that moves with speed u_s. The normal shock wave propagates in the gas at the low pressure section, compressing and heating the gas at rest, initially. Simultaneously, a series of expansion wave propagates toward the high pressure section (not shown in Fig. 2), thinning and cooling the gas (at rest) of the high pressure section.

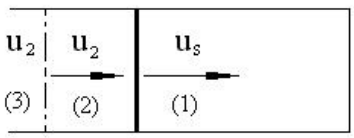

Figure 2. Non-stationary incident normal shock wave.

In $0 < t < t_1$, Fig. 2, the compressed gas at pressure p_2, heated at temperature T_2, in irreversible process s_2, moves with speed u_2, in the direction of shock wave. Similarly, the rarefied gas at pressure p_3, cooled at temperature T_3, in

isentropic process s_3, moves with speed u_3, accelerating the gas toward the shock wave (not shown in Fig. 3). The front of the expansion wave moves at the speed of sound a_4 of the gas in the high-pressure reservoir, while the tail of the expansion wave moves at the speed u_2 of the gas which has experienced the passage of the shock wave, originated in the low-pressure section. From this balance one may concluded $p_2 = p_3$ and $u_2 = u_3$. However, $T_2 \neq T_3$ and $s_2 \neq s_3$. Consequently, a discontinuity, named by contact surface is established, separating the compressed and heated gas by the shock wave and the rarefied and cooled gas by the expansion wave, and the contact surface moves at the same speed of the gas behind the shock wave, $u_2 = u_3$, with pressure $p_2 = p_3$.

In $t = t_1$, Fig. 3, the shock wave reaches the closed end wall, of the low pressure section, and the wave is reflected totally. After a while, the front the expansion wave reaches the closed end wall, of the high pressure section and the wave is reflected totally (not shown in Fig. 3).

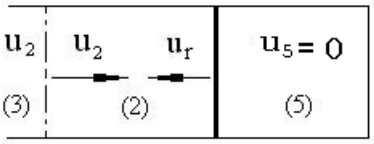

Figure 3. Non-stationary reflected Shock Wave.

In $t = t_2$, Fig. 1, the reflected normal shock wave interacts with the contact surface. The gas between the shock wave and contact surface, from the gas in the low pressure reservoir, induced by the passage of the shock wave, has a constant speed, u_2, constant pressure, p_2, constant temperature, T_2, and constant density, ρ_2. Consequently, this gas may be used in the study related to high speed flow (gas dynamic research). The useful test time of the gas in the flow conditions (2) is estimated by the interaction of the reflected shock wave with the contact surface, Fig. 1, $t = t_2$.

The one-dimensional incident shock wave moving into a stationary gas and the reflect shock wave mode may be used to calculate the flow conditions in the shock tube and the flow over the test model, Fig. 1.

3. SHOCK TUBE MODELING

As the normal shock wave propagates into the low pressure region (driven section) with velocity u_s, it increases the pressure of the gas behind the shock wave and induces a mass motion with velocity u_2. The contact surface between driver and driven gases moves with velocity u_2 and pressure p_2. The expansion wave propagates to the high pressure region (driver section), smoothly and continuously decreasing its pressure to the lower value p_2 behind the expansion wave.

The governing flow equations for the one dimensional incident shock wave are given by

continuity: $\rho_1 u_s = \rho_2 (u_s - u_2)$ (1)

momentum: $p_1 + \rho_1 u_s^2 = p_2 + \rho_2 (u_s - u_2)^2$ (2)

energy: $h_1 + \frac{1}{2} u_s^2 = h_2 + \frac{1}{2} (u_s - u_2)^2$ (3)

equation of state: $h_2 = h_2 (p_2, \rho_2)$ (4)

Once the conditions after the incident shock wave are determined, the conditions existing in the reflected normal shock wave can be found. The incident shock wave is totally reflected, so $u_5 = 0$.

The governing flow equations, for the one-dimensional reflected shock are given by

continuity: $\rho_2 (u_2 + u_r) = \rho_5 u_r$ (5)

momentum: $p_2 + \rho_2 (u_2 + u_r)^2 = p_5 + \rho_5 u_r^2$ (6)

energy: $h_2 + \frac{1}{2}(u_2 + u_r)^2 = h_5 + \frac{1}{2}u_r^2$ (7)

equation of state: $h_5 = h_5(p_5, \rho_5)$ (8)

If the conditions achieved in the shock tube are high enough to produce dissociation, ionization or even recombination, the real gas equation must be used; otherwise the calorically perfect gas equation is used, $p = \rho R T$. For the calorically perfect gas assumption the properties downstream of the shock wave are a function only of the shock wave Mach number and the properties upstream of the shock wave. The flow modeling for this particular case is presented. The pressure, density and temperature ratios across the moving shock wave are given, respectively, by

$$\frac{p_2}{p_1} = \frac{2\gamma_1 M_s^2 - (\gamma_1 - 1)}{\gamma_1 + 1} \tag{9}$$

$$\frac{T_2}{T_1} = \frac{p_2}{p_1}\frac{\rho_1}{\rho_2} = \frac{\left[2\gamma_1 M_s^2 - (\gamma_1 - 1)\right]\left[(\gamma_1 - 1)M_s^2 + 2\right]}{(\gamma_1 + 1)^2 M_s^2} \tag{10}$$

$$\frac{\rho_2}{\rho_1} = \frac{(\gamma_1 + 1)M_s^2}{(\gamma_1 - 1)M_s^2 + 2} \tag{11}$$

The induced velocity imparted by the shock wave moving at constant velocity u_2 may be determined by the continuity condition across the shock wave and it is given by

$$u_2 = \frac{2}{\gamma_1 + 1}u_s\left(\frac{M_s^2 - 1}{M_s^2}\right) = \frac{2}{\gamma_1 + 1}a_1\left(M_s - \frac{1}{M_s}\right) \tag{12}$$

where the incident shock wave Mach number is given by $M_s = \frac{u_s}{a_1}$ and $\gamma_1 = \frac{c_p}{c_v}$ is the ratio of the specific heats.

The induced Mach number, after a moving normal shock wave, is given as function of the incident shock Mach number M_s by (Nagamatsu, 1958, 1961)

$$M_2 = \frac{2\left(M_s^2 - 1\right)}{\sqrt{\left[(\gamma_1 - 1)M_s^2 + 2\right]\left[2\gamma_1 M_s^2 - (\gamma_1 - 1)\right]}} \tag{13}$$

Simultaneously, a rarefaction wave propagates into the high pressure driver tube. Assuming isentropic expansion the pressure ratio in this region is given by

$$\frac{p_4}{p_3} = \left(\frac{a_4}{a_3}\right)^{\frac{2\gamma_4}{\gamma_4 - 1}} \tag{14}$$

The conditions relating the gas states on both sides of the contact surface are that the velocity and pressure are constant across the contact surface. They are given by $u_2 = u_3$ and $p_2 = p_3$. The driver to driven pressure ratio is given by

$$\frac{p_4}{p_1} = \frac{p_2}{p_1}\left\{1 - \left[\frac{a_1(\gamma_4 - 1)}{a_4(\gamma_1 + 1)}\right]\left[M_s - \frac{1}{M_s}\right]\right\}^{-\frac{2\gamma_4}{(\gamma_4 - 1)}} \tag{15}$$

After the incident shock wave arrives at the end of the driven tube, the gas is brought to rest, the shock wave is reflected, and the temperature and the pressure of the gas after the reflected shock wave are increased. The reflected shock wave produces an induced flow velocity equal and opposite to u_2 in order to bring the gas to rest after the

reflected shock wave. The induced Mach number after a moving normal shock wave is given as a function of the reflected shock Mach number by (Nagamatsu, 1958, 1961)

$$M_2 = \frac{u_2}{a_2} = \frac{2}{\gamma_1 + 1}\left(M_r - \frac{1}{M_r} \right) \tag{16}$$

The reflected shock Mach number may be written as a function of the incident shock Mach number as

$$\frac{M_r}{M_r^2 - 1} = \frac{M_s}{M_s^2 - 1}\sqrt{1 + \frac{2(\gamma_1 - 1)}{(\gamma_1 + 1)^2}\left(M_s^2 - 1\right)\left((\gamma_1 + 1)\frac{1}{M_s^2}\right)} \tag{17}$$

An iterative procedure must be used to solve the implicit equation for the reflected shock Mach number. Pressure, density and temperature after the reflected shock Mach number are given, respectively, by

$$\frac{p_5}{p_2} = \frac{2\gamma_1 M_r^2 - (\gamma_1 - 1)}{\gamma_1 + 1} \tag{18}$$

$$\frac{T_5}{T_2} = \frac{p_5}{p_2}\frac{\rho_2}{\rho_5} = \frac{\left[2\gamma_1 M_r^2 - (\gamma_1 - 1)\right]\ \left[(\gamma_1 - 1)M_r^2 + 2\right]}{(\gamma_1 + 1)^2 M_r^2} \tag{19}$$

$$\frac{\rho_5}{\rho_2} = \frac{(\gamma_1 + 1)M_r^2}{(\gamma_1 - 1)M_r^2 + 2} \tag{20}$$

4. THEORETICAL ANALYSIS

For a calorically perfect gas; pressure, temperature and density ratios across a non-stationary incident shock wave are functions only the incident shock Mach number M_s and the ratio of specific heats γ_1 of the existent gas in the driven section, Eqs. (9) to (11), respectively. Such behavior is showing in Figs. 4 to 6.

Knowing the initial conditions of the static properties (p_1 , T_1 , ρ_1) of the calorically perfect gas (γ_1) at rest in the driven section of the shock tube, one may determine by the Eqs. (9) to (11), the properties of the gas behind the non-stationary shock wave. For high-temperature conditions produced by the strong shock waves (about Mach numbers higher than 7 or a velocity higher than 2 km/s) (Anderson, 1990), the equations must be modified to include the real gas effects, given by the eq. (4) (Nagamatsu, 1958, 1961).

It is important to note that for a calorically perfect gas the static properties measured (pressure, temperature and density ratios) with the respect to the moving incident shock wave are the same as the static properties measured (pressure, temperature and density ratios) with the respect to the a stationary shock wave (Chapman and Walker, 1971).

Figures 4 to 6 show as incident Mach number M_s increases to infinite ∞ , the pressure and temperature ratios go to infinite but density ratio approaches to a finite value (6 for air as calorically perfect gas), as the following equations:

$$\lim_{M_s \to \infty}\left(\frac{p_2}{p_1} \right) = \frac{2\gamma_1 M_s^2 - (\gamma_1 - 1)}{\gamma_1 + 1} = \infty \tag{21}$$

$$\lim_{M_s \to \infty}\left(\frac{T_2}{T_1} \right) = \frac{\left[2\gamma_1 M_s^2 - (\gamma_1 - 1)\right]\ \left[(\gamma_1 - 1)M_s^2 + 2\right]}{(\gamma_1 + 1)^2 M_s^2} = \infty \tag{22}$$

$$\lim_{M_s \to \infty}\left(\frac{\rho_2}{\rho_1} \right) = \frac{(\gamma_1 + 1)M_s^2}{(\gamma_1 - 1)M_s^2 + 2} = \frac{(\gamma_1 + 1)}{(\gamma_1 - 1)} \tag{23}$$

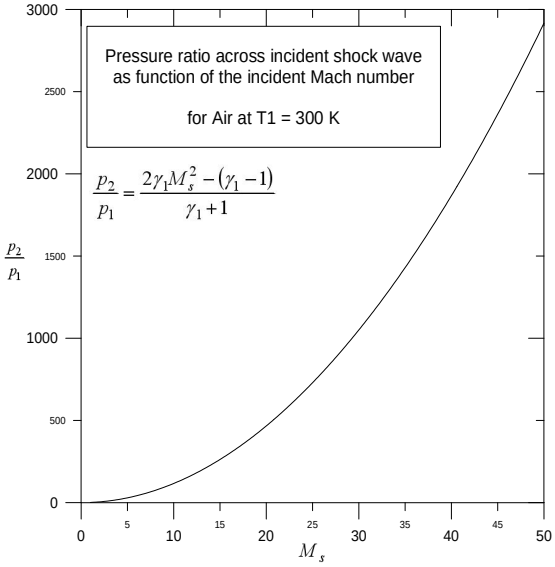

Figure 4. Pressure ratio across incident shock wave.

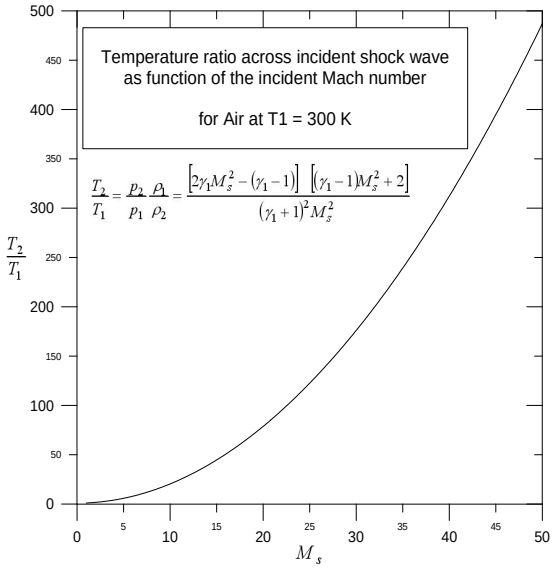

Figure 5. Temperature ratio across incident shock wave.

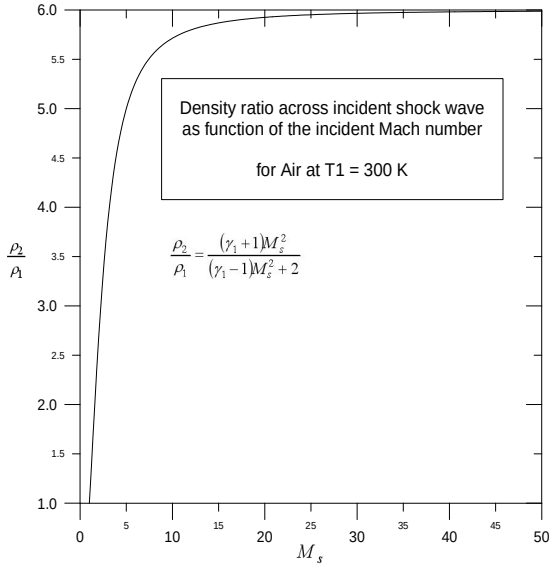

Figure 6. Density ratio across incident shock wave.

For a calorically perfect gas the flow Mach number behind the non-stationary shock wave, Eq. (13), is a function only the incident shock Mach number M_s and the ratio of specific heats γ_1 of the existent gas in the driven section, which behavior is shown in Fig. 7.

Again, it is important to note that for a calorically perfect gas the flow Mach number behind the stationary shock wave is always lower than 1. However, Fig. 7 shows the flow Mach number behind the non-stationary shock wave approaches to 1.89 as incident Mach number M_s increases to infinite ∞ . Also, the limiting case for flow Mach number behind the non-stationary shock wave approaches to finite value, 1.89 for air, Eq. (24).

$$\lim_{M_s \to \infty} (M_2) = \frac{2\left(M_s^2 - 1\right)}{\sqrt{\left[(\gamma_1 - 1)M_s^2 + 2\right]\ \left[2\gamma_1 M_s^2 - (\gamma_1 - 1)\right]}} = \sqrt{\frac{2}{\gamma_1(\gamma_1 - 1)}} \tag{24}$$

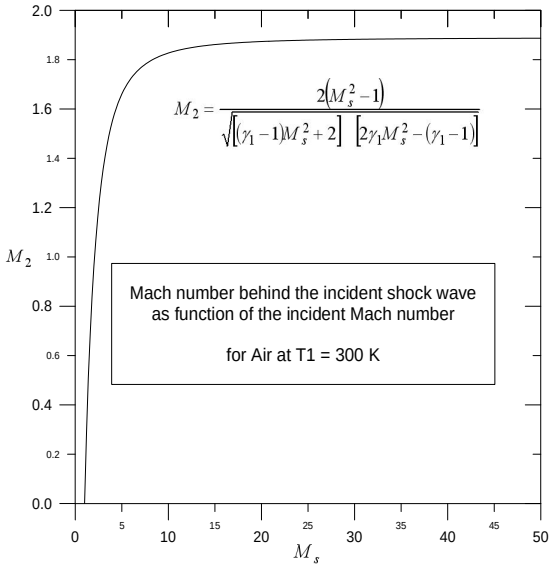

Figure 7. Mach number behind incident shock wave.

Therefore, experimental investigations using calorically perfect air gas in the driven section of the constant-area shock tubes is possible only at low supersonic flow Mach numbers (behind the normal shock wave). The shock tube technique is limited to the flow Mach number that can be attained in the heated gas between the shock wave and the contact surface. For a diatomic gas (air) with a constant value for the ratio of the specific heats γ_1 of 1.4, the limiting flow Mach number after the incident shock wave is only 1.89 (Nagamatsu, 1958, 1961; Anderson 1990).

Finally, by knowing the initial conditions of the gas in the driver and driven sections, the driver to driven pressure ratio (diaphragm pressure ratio), p_4/p_1, determines the strengths of the incident shock and the expansion waves that are established after the diaphragm is broken. For a given calorically perfect gas at the driven section, higher driver temperature or low-molecular-weight driver gas than the driven gas maximizes the incident shock strength.

5. IEAv SHOCK TUBE

The objective of the Prof. Henry T. Nagamatsu Laboratory of Aerothermodynamics and Hypersonics is the development of the hypersonic experimental investigations to simulate the fly conditions of the aerospace vehicle by using the three Pulsed Hypersonic Wind Tunnels, known as Hypersonic Shock Tunnels, Fig. 9.

The main application of the IEAv 68.5-mm Low Pressure Shock Tube, Fig. 9, designed by Miranda and Jardim (1961) is the dynamic calibration of the pressure transducers and the heat transfer gauges. The low pressure shock tube is able to produce shock waves up to Mach numbers 3 and 5 with air and helium, respectively, in the driver section, for a shorter test time of about 50 to 500 microseconds. The minimum pressure in the driven section is on the order of 0.0132 atm (10 mm of Hg) and the maximum pressure in the driver section, due to structural safety limitations, is 70 atm.

Figure 8. Prof. Henry T. Nagamatsu Laboratory of Aerothermodynamics and Hypersonics. Hypersonic Shock Tunnel T1 (next to the right wall), Hypersonic Shock Tunnel T2 (visible at the left of the Hypersonic Shock Tunnel T3).

Figure 9. The IEAv Shock Tube.

The material used in the driver and driven sections is a thin-walled steel pipe with 68.5-mm internal diameter. The driver and driven sections are 517 mm. long and 2,873.4 mm. long, respectively, Fig. 10 The test may be placed at the end or close to the end of the driven section. Instrumentation ports as well as load and/or vacuum ports are provided along the driver and driven sections. The ports close to the end of the driven section are used mainly to install the pressure transducers to measure the shock wave strength and to monitor the shock wave transit time.

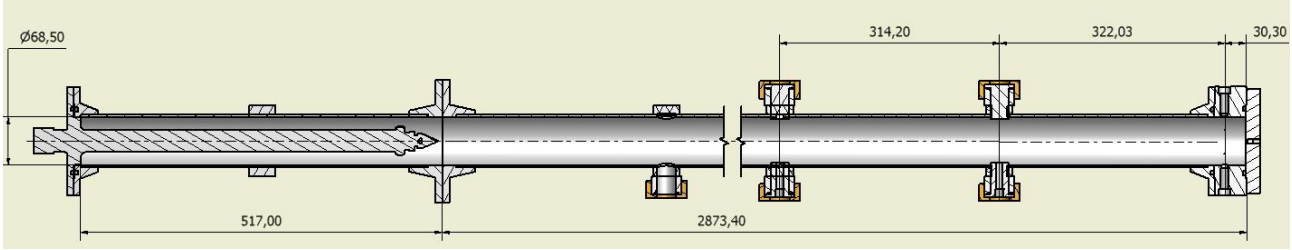

Figure 10. The IEAv Shock Tube characteristics.

The diaphragms involve several materials of various thickness and are chosen according to the pressure difference between the driver and driven sections, $p_4 - p_1$. The entire range in strength of operating pressure is covered by the

following diaphragm materials: very thin-film plastic (popular cellophane supermarket bags), thin-film plastic sheet with about 0.02-mm. thickness, and 0.1 to 0.5-mm. thick aluminum sheet.

The detection of the passage of the shock wave is made through the use of two pressure transducers mounted on instrumentation plugs, 314.20-mm. apart, and kept flush with the shock tube inner wall, Fig. 10.

For short test times the pressure and the heat transfer measurement techniques have to be suited for transient conditions with a response time fast enough to trace variations caused by changing flow conditions.

It is well known that for an experiment to take place all data acquisition instrumentations must be fully operational, that is, it must be able to collect data properly and with as minimal errors as possible. For this purpose, before experiments can be carried out on the actual model which will be inserted in the Hypersonic Shock Tunnels, a calibration is an important step to take place.

Both the pressure transducers and the thin-film Platinum heat gages may be dynamically calibrated in the IEAv 68.5-mm. diameter low-pressure shock tube, under certain known pressure conditions. The calibration process, for the pressure transducer, is to find the relation between the mechanical pressure and its electrical output voltage, Fig. 11 (left) (Damião et al., 2010) and for the thin-film heat gages the calibration is to find the heat gage constant, Fig. 11 (right).

Since the fifties years, various research groups have been developed fast response heat gages to measure heat transfer rates (Nagamatsu and Geiger, 1957; Olivier et al., 1992; Leite and Toro, 2001; Toro and Leite, 2002; Toro et al., 2008). The thin-film resistance thermometer (or thin-film heat gages) consists of a very thin metal film (gold, platinum, rhodium) applied to a backing substrate material of low thermal conductive (pyrex, alumina, macor). Film depositing techniques include platinum sputtering, evaporation under vacuum of gold, platinum and rhodium, or simply painting with appropriate paints, which are then baked at high temperatures. The film thickness has normally a few microns. Their response time is on the order of one microsecond, ideal for the short test times found in shock tubes and shock tunnels.

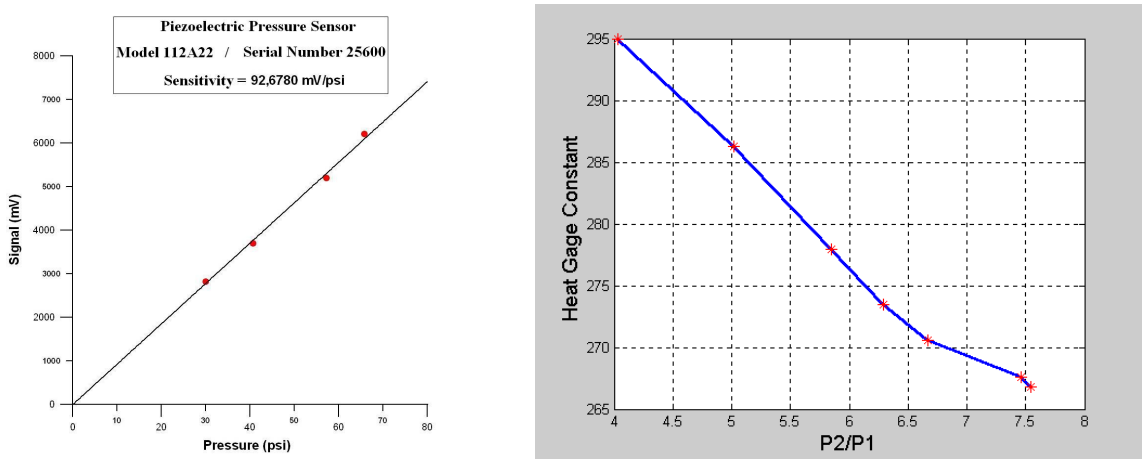

Figure 11. Example of the pressure (left) and thin-film Platinum heat gage (right) calibration curves obtained in the IEAv 68.5-mm Low Pressure Shock Tube.

5. CONCLUSION

Shock tubes have been widely developed since the early 1950s as a powerful laboratory short duration tool to study the high speed and high temperature phenomena in compressible gases.

The shock tube operation, flow modeling and theoretical analysis are presented for the constant area shock tube, which consists basically of driver and driven sections, separated by a single thin diaphragm.

For a calorically perfect air pressure, temperature density ratios across a non-stationary incident shock wave as well as the flow Mach number behind a moving incident shock wave are presented as functions only the incident shock Mach number and the ratio of specific heats of the existent gas in the driven section.

The IEAv 68.5-mm diameter low pressure shock tube, of the Prof. Henry T. Nagamatsu Laboratory of Aerothermodynamics and Hypersonics, which is able to produce flow Mach numbers up to 3 and 5 with air and helium, respectively, in the driver section, for a shorter test time of about 50 to 500 microseconds, is used to the dynamic calibration of the pressure transducers and the thin film Platinum heat transfer gauges.

6. ACKNOWLEDGEMENTS

The third author would like to express his gratitude to the Financiadora de Estudos e Projetos (FINEP, project nº 0445/07, grant # 01.08.0365.00) and Conselho Nacional de Desenvolvimento Científico e Tecnológico (CNPq, process

nº 520017/2009-9) their continued support. Also, acknowledgment is due to the CNPq for the financial support of the two first authors (grant # 181294/2010-9 and grant # 380821/2009-5, respectively). Finally, the authors would like to thank to Alexandre Damião Araujo and Thiago Victor Cordeiro Marcos (CNPq grant # 380823/2009-8) for their useful help in the Shock Tube operation. Special thanks are due to José Brosler Channes Junior for his help in the synchronization event along with Shock Tube.

7. REFERENCES

Anderson Jr., J. A., 1990, "Modern Compressible Flow, The Historical Perspective" McGraw-Hill, Inc., 2nd edition.

Chapman, A. J. and Walker, W. F., 1971, "Introductory Gas Dynamic", H R W Series in Mechanical Engineering, Holt, Rinheart and Winston , Inc.

Damião, A. A. Toro, P. G. P., Minucci, M. A. S., Marcos, T. V. C., Romanelli Pinto, D. and Mantovani, A. F., 2010, "Calibration Methodology for Piezoelectric Pressure Transducers using Supersonic Shock Tubes", 13th Brazilian Congress of Thermal Sciences and Engineering (ENCIT 2010), Uberlândia, Brazil.

Glass, I.I. and Hall, J.G., 1959, Shock Tubes". Handbook of Supersonic Aerodynamics, section 18. Navord Report 1488 (vol. 6).

Leite, V. S. F. O. and Toro, P. G. P., 2001, "Construction and Calibration Procedure of Thin-Film Heat Gages", 16th Brazilian Congress of Mechanical Engineering (COBEM, 2001), Uberlândia, Brazil.

Lukasiewicz, J., 1952, "Shock Tube Theory and Applications". National Aeronautical Establishment, Rept. 15, Otawwa, Canada.

Miranda, A. T., Jardim, L. G., 1961, "Projeto e Construção de um Tubo de Choque". Trabalho de Graduação. ITA.

Nagamatsu, H. T. and Geiger, R. E., 1957, "A Fast Response Device for Measuring Heat Transfer", Proceedings of the 2nd Annual Seminar, Schenectady, New York.

Nagamatsu, H. T., 1958, "Shock Tube Technology and Design", Report No. 58-RL-2107, General Electric Research Laboratory, Schenectady, New York.

Nagamatsu, H. T., 1961, "Shock Tube Technology and Design". chapter III, Fundamental Data Obtained from Shock Tube Experiments, Editor Antonio Ferri, Pergamon Press, 1961.

Olivier, H., Vetter, M., Jessen, C. and Grönig, H., 1992, "Measurements on Models for Hypersonic Real Gas Conditions", Shock Wave Laboratory, University of Technology Aachen.

Toro, P. G. P and Leite, V. S. F. O., 2002, "Pressure Transducer and Heat Flux Gage Calibration using a Shock Tube", II National Congress of Mechanical Engineering, 2002 (CONEM, 2002), João Pessoa, Brazil.

Toro, P. G. P., Minucci, M. A. S., Menezes Filho, A. C., and Romanelli Pinto, D., 2008, "Sensores de Fluxo de Calor de Filme Fino de Platina". V National Congress of Mechanical Engineering (CONEM, 2008), Salvador, Brazil.

8. RESPONSIBILITY NOTICE

The authors are the only responsible for the printed material included in this paper.